Kinetic-energy distributions of Ar^+ ions photodesorbed from argon multilayers

G. Dujardin, L. Hellner, L. Philippe, M-J. Besnard-Ramage, and P. Cirkel
Laboratoire pour l'Utilisation du Rayonnement Electromagnétique (LURE), Bâtiment 209 D, Université de Paris–Sud, 91405 Orsay Cedex, France and Laboratoire de Photophysique Moléculaire, Bâtiment 213, Université de Paris–Sud, 91405 Orsay Cedex, France
(Received 18 May 1993; revised manuscript received 3 August 1993)

Kinetic energies of Ar^+ ions desorbed by double photoionization at 100 eV from argon layers (from 2 to 20 monolayers) condensed on platinum are measured and compared with predicted values. Unexpected low kinetic energies are explained by a relaxed Coulomb repulsion mechanism. The weakness of the high-kinetic-energy ion signal is considered to be due to the noncrossing of the bound and repulsive potential-energy curves involved in the desorption model.

I. INTRODUCTION

Photon interaction with adsorbed or condensed atoms and molecules can result in the emission of positive ions. Such processes are encountered in a variety of photon-stimulated desorption experiments from solid surfaces[1–3] and in studies on the stability and dynamics of photon-excited clusters.[4] The basic issues are the identification of the repulsive mechanisms leading to the ion ejection and the nature of the competing relaxation processes. Although qualitative models have been proposed,[1–3] no satisfactory understanding of the ion photoemission processes could be achieved so far, mainly due to the lack of experimental information on the energetics of the ejected ions. The aim of this work is to provide such experimental data on the kinetic energy of photodesorbed ions in a simple system where clear assignments of the electronic excitation processes can be made.

We report here kinetic-energy measurements of desorbed ions from condensed rare gases. Rare-gas layers on a metal are chosen because they offer a number of advantages. First, they have well-known electronic excited and ionized states producing ion desorption.[5–9] Second, their lowest ionization potential is high enough ($\simeq 13.8$ eV) so that neutralization by the interatomic Auger effect cannot occur within the adsorbed layer. Earlier attempts to study kinetic energies of photodesorbed ions from more complicated systems[10–12] were handicapped by the unknown nature of the electronic excited states involved in the desorption processes. In the present work, the measurements of ion kinetic energies for various thicknesses of condensed argon (from 2 to 20 monolayers) and for well identified excitation mechanisms will allow us to discuss in details the desorption mechanisms.

II. EXPERIMENT

Synchrotron radiation from Super-ACO (the storage ring at Orsay) is dispersed by a grazing-incidence monochromator with a 2-Å band-pass wavelength. Most of the measurements reported here are carried out at a photon energy of 100 eV with a photon flux of about 10^{12} photons $\times s^{-1}$. The experiments are performed in an ultrahigh-vacuum chamber (base pressure below 5×10^{-11} mbar) equipped with a liquid-helium flow cryostat. Pure argon is condensed at low temperature ($\simeq 15$ K) on a polycrystalline platinum substrate which can be cleaned by resistive heating. The sample thickness is calibrated from photoabsorption measurements through thick samples of condensed argon of which the absorption coefficient is known.[13] The accuracy of the thickness measurement for thin layers is checked by comparing the dependence of the Ar^+-ion yield on film thickness obtained by excitation of exciton pairs with that reported in a separate experiment.[9] Desorbed ions can be mass analyzed through a fixed quadrupole filter. By rotating the sample, desorbed positive ions can also be kinetic-energy analyzed through a separate electrostatic hemispherical analyzer working in a constant-pass energy mode. In this latter case, ions are no longer mass selected. The mass analysis of desorbed ions in then performed before and after each kinetic-energy measurement. It is checked that under our experimental conditions, i.e., photon excitation energy of 100 eV and sample thickness lower or equal to 20 monolayers, the desorption of Ar^+ ions accounts for more than 95% of the total amount of desorbed ions. Other observed desorbed ions such as Ar_2^+, Ar_3^+, Ar^{2+}, H^+ have a negligible intensity. Ions are detected along the sample normal with an angular acceptance of about 6°.

Kinetic energies measured through the electrostatic analyzer are relative to the vacuum level of the analyzer ($E_{\rm kin}^{\rm anal}$) and have to be corrected for the different contact potentials of the sample and of the analyzer in order to get kinetic energies relative to the vacuum level of the sample ($E_{\rm kin}^{\rm sample}$). The relation between $E_{\rm kin}^{\rm anal}$ and $E_{\rm kin}^{\rm sample}$ is then

$$E_{\rm kin}^{\rm sample}=E_{\rm kin}^{\rm anal}+\phi_s-\phi_D-V_s\ , \tag{1}$$

where ϕ_s and ϕ_D are the sample and detector sample work functions, respectively, and V_s is the bias voltage of the sample. A somewhat different formula was considered by Kelber *et al.*,[10] who used the same formula for electrons and positively charged ions. It turns out, however, that the different sample and analyzer work func-

tions are expected to have opposite effects on the kinetic energy of negatively and positively charged particles. From separate photoemission experiments, ϕ_D is known to be 4.3 (± 0.1) eV. By measuring the "cutoff" energy of photoelectrons emitted from the sample, ϕ_s is obtained at 4.3 (± 0.1) eV which is by chance the same value as ϕ_D. Correcting the measured kinetic energies by $\phi_s - \phi_D$ introduces an uncertainty of about 0.2 eV. Furthermore, ϕ_s may depend on the adsorbate thickness although in our particular case ϕ_s was constant within experimental uncertainties. Another method was then tried in order to obtain directly absolute values of $E_{\text{kin}}^{\text{sample}}$. For that purpose we assumed that the kinetic-energy distribution is extending down to zero values of $E_{\text{kin}}^{\text{sample}}$. By correcting with the known energy resolution of the analyzer, the lowest measured value of $E_{\text{kin}}^{\text{sample}}$ was then ascribed to zero.

Reported kinetic-energy distributions of ions are obtained with $V_S = 3$ eV and are unchanged for higher values of V_S. For lower values the kinetic-energy distributions are somewhat dependent on V_S indicating that the transmission of the analyzer is not constant for kinetic energies below 3 eV. From ion trajectory simulations, we checked that applying a +3-eV bias potential to the sample is of negligible effect on the recorded kinetic-energy distributions due to the small collection solid angle of our analyzer.

III. RESULTS AND DISCUSSION

Kinetic-energy distributions of Ar^+ ions desorbing from Ar layers of different thickness are shown in Fig. 1. The photon excitation energy of 100 eV is chosen in order to ensure that the primary electronic excitation process producing ion desorption is double ionization,[5] i.e., the formation of a doubly charged Ar^{2+} ion. At this photon energy the role of double ionization is indeed maximum since single ionization does not produce any ion desorption and the cross section of other ionization processes such as formation of ionic satellite states or triple ionization are comparatively negligible.[5,14] Most of the Ar^+ desorbed ions are believed to result from direct photon excitation since the recording of the Ar^+ ion intensity as a function of the photon energy over the 20–100-eV energy range[5,14] shows no evidence of desorption processes induced by secondary electrons from the substrate or from the condensed atoms. Nevertheless, the desorption of Ar^+ ions produced by secondary electrons with high kinetic energies would be also dominated by double ionization of condensed Ar atoms. The kinetic-energy calibration of curves in Fig. 1 is obtained by using formula (1) of the preceding section. By improving the energy resolution of the analyzer, we also recorded the two kinetic-energy distribution curves shown in Fig. 2. These curves are obtained with 5 monolayers of condensed argon and photon energies of 100 and 40 eV. In Fig. 2, the energy calibration is done according to the second method described in Sec. II, i.e., by assuming that the lowest measured kinetic energy is zero and by taking into account the 0.2-eV energy resolution of the analyzer. As mentioned before, the two methods for energy calibration give similar results. The kinetic-energy distribution at a photon energy of 40 eV could be obtained only for a 5-monolayer thickness since at lower thicknesses the desorbed ion mass spectrum showed a large amount of impurities which were not observed at a photon energy of 100 eV. Further experiments at a photon energy of 40 eV would then require both kinetic energy and mass analysis of desorbed ions in order to be sure that the recorded kinetic-energy distribution is that of Ar^+ ions.

Kinetic energies of desorbed Ar^+ ions as seen in the curves of Fig. 1 are much smaller than what is predicted from the direct Coulomb repulsion model.[5] Within this model the initially produced doubly charged Ar^{2+} ions are believed to undergo a charge exchange with a neighbor Ar atom followed by a rapid Coulomb repulsion between the two singly charged Ar^+ ions. The total kinetic

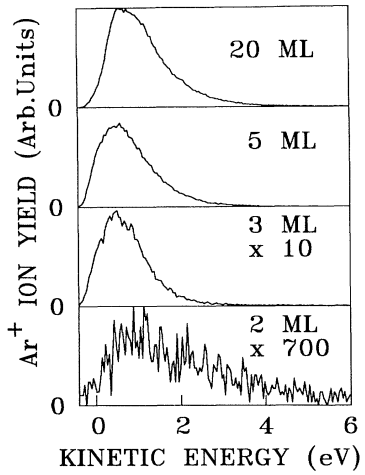

FIG. 1. Kinetic-energy distributions of Ar^+ ions desorbed from argon layers of various thicknesses. The photon excitation energy is 100 eV. The energy resolution of the analyzer is about 0.4 eV.

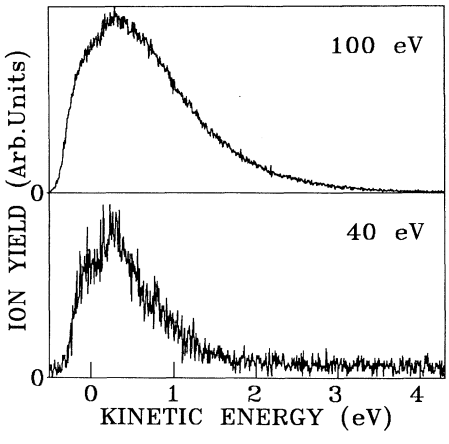

FIG. 2. Kinetic-energy distributions of Ar^+ ions desorbed from 5 monolayers of condensed argon. The energy resolution of the analyzer is about 0.2 eV. The photon excitation energy is 100 eV (upper curve) and 40 eV (lower curve).

energy released is then expected to be 12.2 eV, i.e., the difference between the formation energy of Ar^{2+} at 39.8 eV (Ref. 15) and that of $Ar^+ + Ar^+$ at 2×13.8 eV $= 27.6$ eV.[15] Assuming that each Ar^+ ion takes half of this energy (6.1 eV), the desorbed Ar^+ ion would leave the sample with a kinetic energy of about 4.1 eV after passing over the potential-energy barrier of about 2 eV due to the difference between the ionization energy of argon in the solid (13.8 eV) and in the vacuum (15.8 eV). The actual height of this energy barrier may be less than 2 eV if the Ar^+ ions are produced on the sample surface where the ionization energy of argon is closer to that of argon in the vacuum. The Coulomb repulsion model is schematically represented in Fig. 3. The potential-energy curves are taken from the recent calculations of Cachoncinlle *et al.*[16] by assuming that the atom-atom interactions calculated for the ionic excimer Ar_2^{2+} are not modified in the argon layers. Only potential-energy curves with the $^3\Pi_g$ and $^1\Sigma_u^+$ symmetry are considered in Fig. 3, however potential-energy curves with other symmetries are qualitatively similar.[16] From the diagram of Fig. 3, the desorption of Ar^+ is considered to occur by tunneling from the $Ar + Ar^{2+}$ potential-energy curve to the $Ar^+ + Ar^+$ one. The expected kinetic energy of 4.1 eV differs markedly from the kinetic-energy distributions of Fig. 1 which have a maximum around 0.5 eV and hardly extend beyond 2 eV except for the thinnest layer [2 monolayers (ML's)] which shows a much broader distribution. From this result, it would be tempting to consider an alternative desorption model[7] in which the doubly charged Ar_2^{2+} ionomer would capture an electron leading to the less repulsive singly charged Ar_2^+ ionomers. However, this process is not likely to occur since the Ar_2^+ potential-energy curves[17] are not repulsive enough to allow the Ar^+ atom to overcome the 2-eV energy barrier before desorption.

Considering in Fig. 1 the kinetic-energy distribution of the 2-monolayer system we note that the high-energy part lying in the 3–4-eV range is quite compatible with the previously predicted 4.1-eV kinetic energy. We emphasize that this high-energy tail of the kinetic-energy distribution also exists for thicker samples although this is not easily seen in Fig. 1 due to the occurrence of a much larger signal at low kinetic energies of which the intensity strongly increases with the sample thickness. It is difficult to ascertain that two separate desorption mechanisms, one corresponding to high kinetic energies ($\simeq 4.1$ eV) and the other one to low kinetic energies ($\simeq 0.5$ eV), account for the observed kinetic-energy distributions of Fig. 1. If this were the case, the first mechanism, mainly visible in the 2-ML sample and giving rise to high kinetic energies (3–4 eV), would consist in a direct tunneling to the $Ar^+ + Ar^+$ repulsive potential-energy curve. This mechanism will be referred to in the following as the direct Coulomb repulsion mechanism. In any case its intensity is quite weak, most probably due to an unefficient tunneling to the $Ar^+ + Ar^+$ curve and to a rapid Auger neutralization of Ar^{2+} and/or Ar^+ ions. By contrast the dominant mechanism gives rise to low kinetic energies around 0.5 eV. Its intensity exponentially increases with the sample thickness, indicating that this slower desorption is strongly perturbed by interactions with the platinum substrate for argon layers thinner than 5 monolayers. This desorption mechanism which will be called the relaxed Coulomb repulsion mechanism is also ascribed to a transition from the $Ar + Ar^{2+}$ potential-energy curve to the $Ar^+ + Ar^+$ one. However, only a small amount of the initial electronic excitation energy is transferred to the kinetic energy of the Ar^+ ions. This may be due to the conversion of the initial electronic energy into the evaporation of neutral atoms or excitation of phonons by collisions or by vibronic coupling. In this respect, the diatomic picture of Fig. 3 is oversimplified and it would be worthwhile to consider the dynamic response of larger systems including many more argon atoms. This would also enable us to take into account the screening effect by other argon atoms which is expected to weaken the Coulomb repulsion between Ar^+ ions. An alternative explanation would consist in a radiative transition from the $Ar + Ar^{2+}$ potential-energy curve to the $Ar^+ + Ar^+$ one (see Fig. 3). Such an emission has been discussed recently by Cachoncinlle *et al.*[16] and should occur as a broadband around 183 nm ($\simeq 6.8$ eV). This would reduce the total kinetic energy released from 12.2 to 5.4 eV. Within the same diatomic model that we previously discussed, this would result in the desorption of Ar^+ ions having a kinetic energy of 0.7 eV. This energy coincides with that experimentally observed as the center of the low-energy broadbands in Fig. 1. It is striking that the low-energy part of the kinetic-energy distributions of desorbed Ar^+ ions is well explained by a vertical transition from the bound part of the upper $Ar + Ar^{2+}$ potential-energy curve to the repulsive $Ar^+ + Ar^+$ curve. This is somewhat similar to the case encountered for neutral desorption from condensed rare gases[18] although different ionic potential-energy curves are involved here. We note that the relaxation of the system via a vertical transition is in favor of the emission

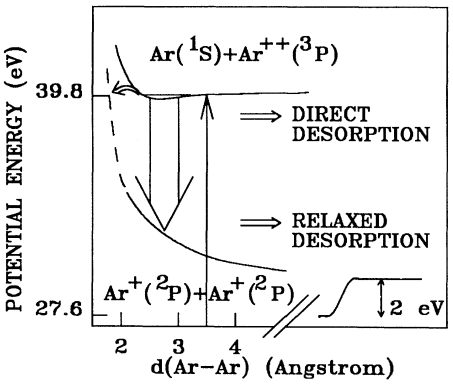

FIG. 3. Argon-layer potential-energy diagram illustrating the direct Coulomb repulsion and relaxed Coulomb repulsion desorption mechanisms. The $Ar + Ar^{2+}$ ($^3\Pi_g$) and $Ar^+ + Ar^+$ ($^1\Sigma_u^+$) potential-energy curves in the full line are taken from Cachoncinlle *et al.* (Ref. 16). The potential-energy barrier of about 2 eV at long distance for Ar^+ ions to escape from the argon layer is indicated. The $Ar^+ + Ar^+$ limit energy is that of the argon layer.

mechanism rather than the excitation of phonons since in this latter case the electronic transition is not necessarily vertical.

The intensity of the direct Coulomb repulsion process (high kinetic energies) is much smaller than that of the relaxed Coulomb repulsion process (low kinetic energies) as long as the sample thickness is above 2 monolayers. This is somewhat surprising since the relaxed process is expected *a priori* to be slower than the direct process. It seems, however, from the calculations of Cachoncinlle *et al.*[16] (see Fig. 3) that the $Ar+Ar^{2+}$ and $Ar^{+}+Ar^{+}$ potential-energy curves are noncrossing, which makes the direct transition much less probable.

As seen in Fig. 1, the intensity of the relaxed Coulomb repulsion process increases very rapidly with the sample thickness up to about 5 monolayers and reaches a saturation for thicker layers. This clearly cannot be ascribed to a simple additive effect of the various monolayers and most probably originates from the neutralization by the platinum substrate. Assuming that the ion desorption occurs from the outermost monolayer and that Auger neutralization by the platinum is the main quenching effect, one can derive an order of magnitude of the exponential factor b appearing in the Auger neutralization rate $\Gamma(x)=\Gamma_0(x/x0)^2\exp[-b(x-x0)]$.[19] From 2 to 3 monolayers, i.e., for x increasing $\simeq 2.6$ Å,[20] $\Gamma(x)$ has to be divided by a factor 100 in order to get the strong increasing of the ion desorption signal seen in Fig. 1. This leads to a value of $b \simeq 2.3$ Å^{-1} which is quite compatible with expected values.[19] We note that the Auger neutralization may quench the initially produced Ar^{2+} ions as well as the singly charged Ar^{+} ions resulting from the $Ar+Ar^{2+}\rightarrow Ar^{+}+Ar^{+}$ transition. In this latter case, the Auger neutralization is expected to be less effective for high-kinetic-energy ions (direct process) than for low-kinetic-energy Ar^{+} ions (relaxed process). We also emphasize that a complete model should take into account other interactions with the platinum substrate such as the image charge interactions.

It is interesting to compare the kinetic-energy distributions of desorbed Ar^{+} ions (Fig. 1) with those of Ar^{+} ions produced by $2p$ core excitation of argon clusters as reported by Rühl *et al.*[4] The excitation mechanisms are not identical in both cases, however one can reasonably assume that an important part of the $2p$ core excited argon clusters relaxes to doubly charged ionized clusters.[21] Rühl *et al.* reported that the $Ar_2^{+}+Ar^{+}$ ion pairs have a kinetic-energy distribution with a maximum at an unexpectedly low value of 0.7 ± 0.2 eV. Assuming that the Ar^{+} ions take $\frac{2}{3}$ of this kinetic-energy, one obtains a kinetic-energy distribution of the Ar^{+} ions with a maximum at 0.5 eV and a tail of a much reduced intensity extending up to about 4 eV. We note that these results are very similar to those obtained from argon layers, at least the thickest ones where the interaction with the platinum substrate can be neglected. This indicates that the desorption mechanisms that we have discussed for argon layers may also be valid in explaining the dynamics of doubly charged argon clusters.

We emphasize that the proposed ion desorption mechanisms are believed to hold for ion desorption originating from double ionization. Double ionization is expected to play a dominant role in ion desorption not only at high energy (>60 eV) in the valence region but moreover in the $2p$ core excitation region[6] where the formation of doubly charged ions is known in the gas phase to be the dominant relaxation process.[21] However, as mentioned in the Introduction, ion desorption may also be produced at lower excitation energies by other processes such as the formation of exciton pairs or ionic valence satellite states. In these latter cases, different desorption mechanisms should probably be considered.

We showed in Fig. 2 a kinetic-energy distribution of desorbed ions obtained at a photon energy of 40 eV where the dominant excitation process is thought to be the formation of ionic valence satellite states since double photoionization of which the threshold energy is at 39.8 eV is negligible at 40 eV.[5] This kinetic-energy distribution seems to be narrower and have a maximum at a lower energy than the distribution at a photon energy of 100 eV also shown in Fig. 2. However this effect cannot be unambiguously ascribed to the Ar^{+} ion desorption since other impurity ions were also desorbed at a photon energy of 40 eV. Impurity ions (masses 12, 13, and 19) most probably originate from traces of hydrocarbon and water molecules present in the gas inlet system. Their relative intensity is very small at 100 eV where the cross section for Ar^{+} desorption is about 10 times higher than at 40 eV.

IV. CONCLUSION

Single photoionization in condensed multilayers of argon is known to produce no ion desorption whereas double photoionization as well as some other two-electron excitation processes do produce ion desorption.[5] The ion desorption produced by double ionization is thought to be related to a transition from the attractive $Ar+Ar^{2+}$ potential-energy curve to the repulsive $Ar^{+}+Ar^{+}$ one. The strong repulsive character of this $Ar^{+}+Ar^{+}$ curve is expected to provide enough kinetic energy for the ejected Ar^{+} ions to overcome the potential-energy barrier before desorption. On the contrary, the $Ar+Ar^{+}$ potential-energy curve is not repulsive enough to allow any ion desorption. Within this model, the direct Coulomb repulsion process was expected to give rise to an intense signal of Ar^{+} ions having high kinetic energies around 4.1 eV. Such a Coulomb repulsion process has been infered from fragmentation studies of doubly charged molecules[22] and He_2^{2+} dimers[23] where ionic fragments having high kinetic energies were observed.

We presented here measurements of kinetic-energy distributions of desorbed ions from rare-gas layers. The main result is that kinetic energies are much smaller than expected from the Coulomb repulsion model. At a photon energy of 100 eV the kinetic-energy distributions have a maximum around 0.5 eV. This finding is in excellent agreement with measured kinetic energies of ions arising from the fragmentation of multiply charged argon clusters.[4] This is in favor of a relaxed Coulomb repulsion process in which the relaxation preceding the ion desorption would occur either by a radiative electronic relaxa-

tion, by evaporation of neutral atoms, or by excitation of phonons. Recent calculations on the $Ar+Ar^{2+}$ and $Ar^+ + Ar^+$ potential-energy curves[16] indicate that a radiative electronic relaxation may occur. However many more experiments on the detection of possible photon emission or neutral desorption are needed in order to clarify the relaxation mechanisms. From the calculations of Cachoncinlle *et al.*,[16] the lack of high-kinetic-energy desorbed Ar^+ ions arising from a direct Coulomb repulsion seems to be due to the noncrossing of the $Ar+Ar^{2+}$ and $Ar^+ + Ar^+$ potential-energy curves. We think that this is somewhat peculiar to the case of argon. In other condensates the corresponding potential-energy curves may well have a crossing point resulting in high-kinetic-energy desorbed ions.

Kinetic-energy measurements were limited here to a photon excitation energy of 100 eV and to small numbers of argon multilayers for which only Ar^+ ions are desorbed. For other photon energies, thicker samples, and/or other condensates, several ionic species are usually desorbed and the present experimental method cannot be used. In such cases further experiments with simultaneous kinetic energy and mass analysis of photodesorbed ions will be needed.

ACKNOWLEDGMENTS

We thank D. Menzel, P. Feulner, and E. Rühl for very helpful discussions. We also acknowledge the Science program of the E.E.C., Grant No. SC1-CT91-0641.

[1]M. L. Knotek, Rep. Prog. Phys. **47**, 1499 (1984).
[2]Ph. Avouris and R. E. Walkup, Annu. Rev. Phys. Chem. **40**, 198 (1989).
[3]R. A. Baragiola and T. E. Madey, in *Interaction of Charged Particles with Solids and Surfaces,* edited by A. Gras-Marti (Plenum, New York, 1991), p. 313.
[4]E. Rühl, C. Schmale, H. W. Jochims, E. Biller, M. Simon, and H. Baumgartel, J. Chem. Phys. **95**, 6544 (1991).
[5]G. Dujardin, L. Hellner, M.-J. Besnard-Ramage, and R. Azria, Phys. Rev. Lett. **64**, 1289 (1990).
[6]G. Rocker, P. Feulner, R. Scheuerer, L. Zhu, and D. Menzel, Phys. Scr. **41**, 1014 (1990).
[7]D. Menzel, Appl. Phys. A **51**, 163 (1990).
[8]Y. Baba, G. Dujardin, P. Feulner, and D. Menzel, Phys. Rev. Lett. **66**, 3269 (1991).
[9]T. Schwabenthan, R. Scheuerer, E. Hudel, and P. Feulner, Solid State Commun. **80**, 773 (1991).
[10]J. A. Kelber, R. R. Daniels, M. Turowski, G. Margaritondo, N. H. Tolk, and J. S. Kraus, Phys. Rev. B **30**, 4748 (1984).
[11]T. R. Pian, M. M. Traum, J. S. Kraus, N. H. Tolk, N. G. Stoffel, and G. Margaritondo, Surf. Sci. **128**, 13 (1983).
[12]J. A. Yarmoff and S. A. Joyce, Phys. Rev. B **40**, 3143 (1989).
[13]B. Sonntag, in *Rare Gas Solids,* edited by M. L. Klein and J. A. Venables (Academic, New York, 1977), Vol. II, p. 1083.
[14]G. Dujardin, L. Hellner, M.-J. Besnard-Ramage, and L. Philippe (unpublished).
[15]H. W. Biester, M.-J. Besnard, G. Dujardin, L. Hellner, and E. E. Koch, Phys. Rev. Lett. **59**, 1277 (1987).
[16]C. Cachoncinlle, J. M. Pouvesle, G. Durand, and F. Spiegelmann, J. Chem. Phys. **96**, 6085 (1992).
[17]H. V. Böhmer and S. D. Peyeriimhoff, J. Phys. D **3**, 195 (1986).
[18]C. T. Reimann, W. L. Brown, D. E. Grosjean, and M. J. Nowakowski, Phys. Rev. B **45**, 43 (1992).
[19]R. E. Walkup, Ph. Avouris, N. D. Lang, and R. Kawai, Phys. Rev. Lett. **63**, 1972 (1989).
[20]G. L. Pollak, Rev. Mod. Phys. **36**, 748 (1964).
[21]D. M. P. Holland, K. Codling, J. B. West, and G. V. Marr, J. Phys. B **12**, 2465 (1979).
[22]G. Dujardin, S. Leach, O. Dutuit, P. M Guyon, and M. Richard-Viard, Chem. Phys. **88**, 339 (1984).
[23]C. A. Nicolaides, Chem. Phys. Lett. **161**, 547 (1989).